

# Transition between nonsingular vortices in superfluid $^3\text{He-A}$ at zero magnetic field

K. Torizuka, J. P. Pekola, A. J. Manninen, and G. E. Volovik<sup>1)</sup>

*Low Temperature Laboratory, Helsinki University of Technology, 02150 Espoo, Finland*

(Submitted 12 February 1991)

*Pis'ma Zh. Eksp. Teor. Fiz.* Vol. 53, No. 5, 263–268 (1910 March 1991)

Rotating  $^3\text{He-A}$  in zero magnetic field exhibits a new first-order phase transition which was discovered by ultrasonic measurements at high angular velocity,  $\Omega_c \simeq 3$  rad/s. A possible mechanism of the observed phase change, which is related to the surface vortex layer, is discussed.

Two types of continuous vortices have been resolved recently by ultrasonic experiments in  $^3\text{He-A}$ .<sup>1</sup> In each case the singularity in the phase of the Bose condensate is unwound because of the nontrivial topology of the orbital  $\vec{l}$ -vector texture in the soft vortex core. The tiny spin-orbit (dipolar) coupling between  $\vec{l}$  and the magnetic anisotropy vector  $\vec{d}$  is responsible for the difference between these vortices. In a low magnetic field,  $H < H_d$ , where  $H_d$  is the dipolar field of order 2–5 mT, the  $\vec{d}$ -texture is dipole-locked with the  $\vec{l}$ -vector and thus follows the nontrivial topology of  $\vec{l}$ , while in higher fields  $\vec{d}$  is unlocked and has a trivial topology. The high-field doubly quantized vortex, with a soft core on the order of the dipolar length  $\xi_d \sim 10 \mu\text{m}$ , was extensively studied in NMR experiments.<sup>2</sup> The first-order phase transition between the dipole-locked and dipole-unlocked nonsingular vortices occurs at  $H = H_c = 1.4 \text{ mT} \simeq H_d$ , irrespective of the angular velocity  $\Omega$ , at least when  $\Omega$  is in the experimental range between 0 and 3.5 rad/s.<sup>1</sup>

In the present ultrasonic experiment we found another transition in low fields  $H \ll H_d$ , i.e., in the region of the dipole-locked vortices. This change takes place at a relatively high  $\Omega$ : when  $H = 0$ , the critical velocity  $\Omega_c \simeq 3$  rad/s. Our experimental setup was described in Ref. 1. In the present study we measured the attenuation  $\alpha(\Omega)$  of ultrasound pulses at a frequency of 26.8 MHz, propagated along the axis of the cylindrical experimental cell (radius  $R = 3$  mm, height  $L = 4$  mm), which was rotated around its axis in our ROTA2 cryostat.

The new transition, seen in  $\alpha(\Omega)$ , has a number of characteristic but puzzling features:

1. The transition is a first-order transition since hysteresis is observed (see Fig. 1). The attenuation curve, while decelerating, does not follow the curve during acceleration; the latter exhibits a reproducible pronounced change at  $\Omega = \Omega_c$ . The hysteresis indicates that the low-velocity vortices are unstable against high-velocity vortices at  $\Omega > \Omega_c$ , but that the latter are metastable and prevail during deceleration, even when  $\Omega < \Omega_c$ . Other sharp features of the  $\alpha(\Omega)$  curve in Fig. 1 are not related to the new transition: i) The peak downwards at the beginning of acceleration is due to counterflow between the normal and superfluid components before vortices are created; ii) after stopping the cryostat the attenuation increases, because the orienting effect of vortices on the  $\vec{l}$ -texture disappears.

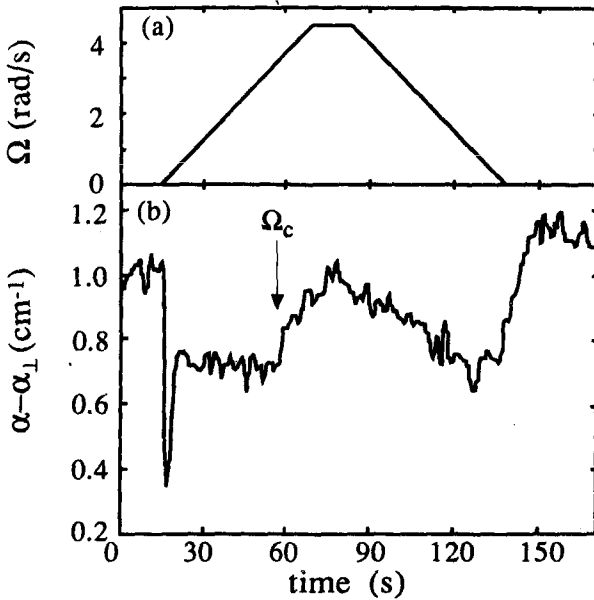


FIG. 1. Attenuation of 26.8-MHz ultrasound in an acceleration-deceleration cycle. Magnetic field  $H \approx 0$  ( $< 0.1$  mT), pressure  $p = 26.0$  bar, and the normalized temperature  $T/T_c = 0.90$ , where  $T_c = 2.4$  mK corresponds to the superfluid transition. The rotation velocity ( $\Omega$ ) is shown vs time in (a); the corresponding attenuation is seen in (b). Here  $\alpha_{\perp}$  is the attenuation level in a strong magnetic field ( $H > H_d$  at  $\Omega = 0$ , when  $\vec{l}$  is perpendicular to the propagation of ultrasound). The transition at  $\Omega_c \approx 3$  rad/s was clearly seen in all our experimental runs.

2. The transition is seen both in measurements during which attenuation is monitored under continuous acceleration (see Fig. 1) and in start-and-stop experiments (see Fig. 2). In the latter method the cryostat was repeatedly accelerated to various final velocities  $\Omega_f$  at which attenuation was recorded.

3. The ultrasound attenuation has a plateau below  $\Omega_c$  for the low-velocity vortices, while for the high-velocity vortices the attenuation always decreases with decreasing  $\Omega$ , even below  $\Omega_c$ .

4.  $\Omega_c$ , as measured from start-and-stop experiments, increase from  $\approx 3$  rad/s to 3.5 rad/s when the pressure is increased from 26.0 bar to 29.3 bar.

In the rest of this paper we discuss our understanding of this transition.

The first-order phase change, with a clear metastability of the high-velocity vortices below  $\Omega_c$  and with instability of the low-velocity vortices above  $\Omega_c$ , rules out an explanation in terms of a transition from the nonsingular dipole-locked vortices, which should exist at low  $\Omega$ , to singular vortices, which should be present at very high angular velocities ( $\approx 30$  rad/s, according to Ref. 3). We believe that it is much more difficult to create singular vortices from a continuous texture, than to produce continuous vorticity from singular vortices.

The fact that sound attenuation has a plateau for the low-velocity vortices and

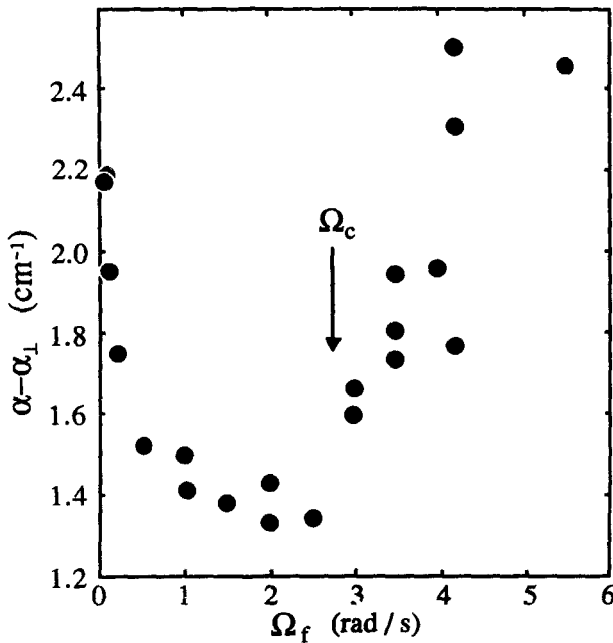


FIG. 2. Ultrasound attenuation measured in start-and-stop experiments under the same experimental condition as in Fig. 1,  $T/T_c = 0.93$ .

increases with  $\Omega$  for the high-velocity vortices (see Figs. 1 and 2) has two consequences: i) For the low-velocity vortices, below  $\Omega_c$ , the  $\hat{l}$ -texture has no internal length scale (such as  $\xi_d$ ), except the size of the primitive vortex cell  $r_V$ . This corresponds to one of the possible periodic dipole-locked textures without an internal length scale,<sup>4</sup> which should exist in the absence of a magnetic field. ii) The high-velocity vortices have an internal length scale, specifically, the size of the region within the cell, where  $\hat{l}$  deviates from the orientation perpendicular to  $\hat{\Omega}$ . This rules out the possibility that the observed transition is between different types of dipole-locked textures. Furthermore, such a change cannot occur at a given  $\Omega$ , since the energy per unit cell does not depend on  $\Omega$  in a vortex texture without an internal length scale.

This leaves the possibility that the high-velocity vortices are dipole-unlocked and nonsingular, i.e., the phase change is of the same origin as the topological transition observed at  $H \approx H_d$ . To understand how the dipole-locked texture in the bulk liquid can lose its stability by acceleration, we consider a scenario which takes into account the fact that singularities are not easily created in a rotating container. This was observed from NMR experiments on rotating  $^3\text{He}$  (see the review article in Ref. 5) which showed that it is difficult to create the singular  $B$ -phase vortices and that nonsingular  $A$ -phase vortices are formed instead of the energetically more advantageous singular vortices.

If it is a general rule that singularities in the order parameter are not created in continuous processes, then one should reconsider the structure of the rotating texture in the  $A$ -phase. The conventional wisdom that this state consists of a regular array of doubly quantized nonsingular vortices suggests that there should be also a regular array of point singularities in the  $\hat{l}$ -vector field on the top and bottom surfaces of the

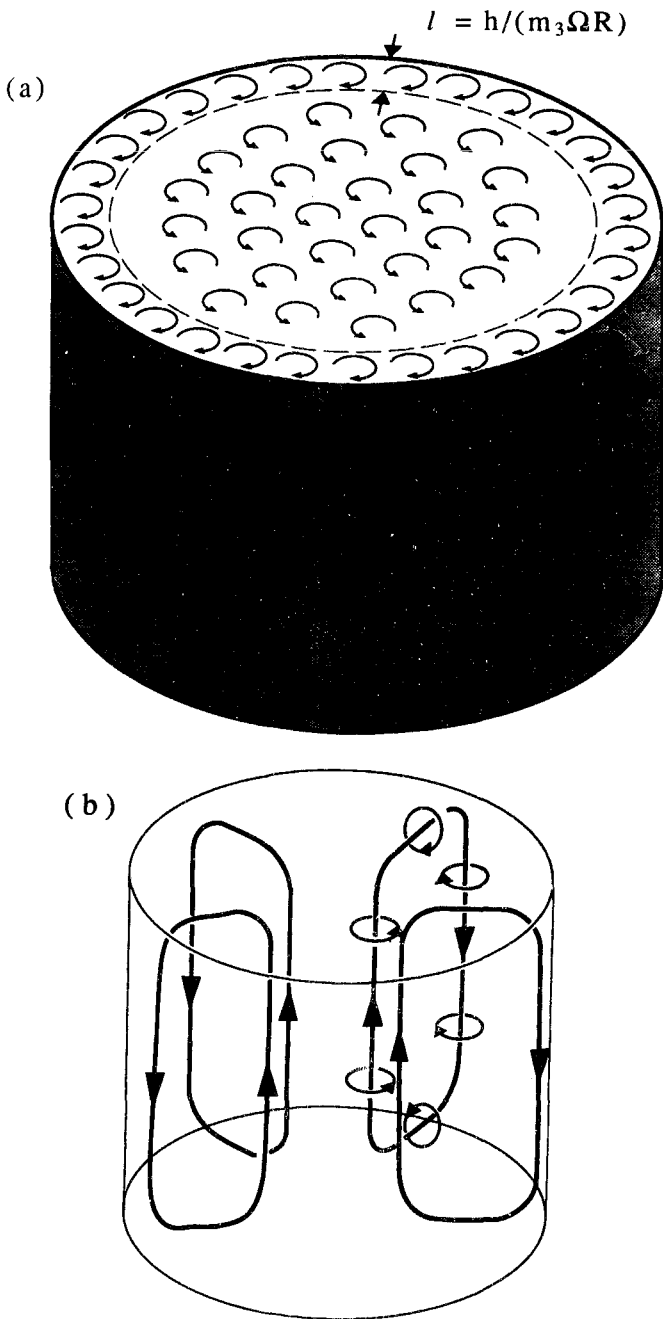


FIG. 3. Schematic illustration of a completely nonsingular vortex texture in the cylindrical experimental vessel: (a) Cross-sectional view of the experimental chamber away from the end plates; there are  $N_v = 30$  vortices in the bulk liquid, where they form a regular array; the same number of opposite vortices are in the surface layer of thickness  $l$ . These vortices form closed loops shown in (b) for  $N_v = 4$ ; vortex filaments are illustrated by thick lines with arrows along the direction of vorticity,  $\text{curl}\vec{v}_s$ ; thin arrows indicate superflow around vortex lines.

rotating container, these boojums<sup>6</sup> are the end points of nonsingular vortices. This is, however, in contradiction with our requirement of the absence of singularities in the rotating vessel.

Let us therefore consider a completely nonsingular distribution of the  $\vec{l}$ -texture, which has the minimum free energy in the rotating vessel. The absence of singularities implies that there is no circulation of  $\vec{v}_s$  around the surface of the vessel, i.e., while  $\langle \vec{v}_s \rangle = \vec{\Omega} \times \vec{r}$  in the bulk liquid, one has  $\langle \vec{v}_s \rangle = 0$  at the surface. The corresponding state is a regular array of conventional doubly quantized vortices in the bulk liquid, with  $\langle \vec{v}_s \rangle = \vec{\Omega} \times \vec{r}$ , which is accompanied by a continuous vortex layer near the surfaces,<sup>6</sup> which compensates for the velocity and produces the condition  $\langle \vec{v}_s \rangle = 0$  on the surface. This layer consists of continuous vortices, whose number  $N_V$  is the same but whose circulation is opposite to the bulk vortices to conserve the circulation (see Fig. 3a). Therefore, the overall topological invariant for the  $\vec{l}$ -texture is zero:  $\int dx dy (\vec{d} \cdot 4\partial_z \vec{l} \times \partial_y \vec{l}) = 0$ , and the same is true for the  $\vec{d}$ -vector field.

Physically, the surface vortices are just a continuation of bulk vortices, when the latter touch the top or the bottom of the rotating vessel, and propagate along the end plates to the side, forming a vortex ring (see Fig. 3b). The vortices in the surface layer are compressed, since the width of this layer for the side walls is<sup>7</sup>  $l = 2\pi R / N_V$ , where  $N_V = \Omega R^2 m_3 / \hbar$  is the number of vortices in the surface layer. Typically, we have  $l = 2 \times 10^{-3}$  cm for  $\Omega = 1$  rad/s and thus comparable to the dipolar length. For the top and bottom plates  $l$  depends on the distance  $r$  from the axis of the vessel:  $l(r) = h / (m_3 \Omega r)$ .

Our ultrasonic experiments in zero field are consistent with the existence of this surface layer of vortices. During continuous acceleration, attenuation caused by the dipole-locked vortices in the bulk liquid should be independent of  $\Omega$ , but, instead,  $\alpha(\Omega)$  reproducibly decreased with increasing  $\Omega$  before reaching the plateau in our start-and-stop experiments (see Fig. 2). The extra attenuation at low velocities is related to the vortex layer on top and bottom surfaces of the vessel: The vortices in these layers are directed perpendicular to the sound propagation and, therefore, the  $\vec{l}$ -vector deviates from its transverse orientation in the bulk liquid, producing the extra attenuation which decreases with  $\Omega$  since the width of the vortex layer decreases as  $1/\Omega$ . Our estimate, using numerical sound attenuation parameters<sup>8</sup> and the value of  $l$  from above, gives the correct order of magnitude for the extra attenuation below  $\Omega_c$ .

Another feature to be compared with our model is the pressure dependence of  $\Omega_c$ . Because the transition should occur when  $l \simeq \xi_d$ , we expect that  $\Omega_c$  is proportional to  $1/\xi_d$ . According to Ref. 8,  $1/\xi_d$  increases about 15% when  $p$  is increased from 26 to 29 bar, which agrees with the observed increase of  $\Omega_c$  from 3 to 3.5 rad/s.

The new phase transition at  $\Omega \simeq 3$  rad/s may now be identified with the dipole-locked-dipole-unlocked transition in vortices at the compressed surface layer, since at this angular velocity the core size of the surface vortices is on the order of the dipolar length, which makes the dipole-unlocked constant  $\vec{d}$ -field more advantageous. This transition then propagates to bulk vortices, which absorb the expelled topological invariant of the  $\vec{d}$ -field.

We thank J. M. Kyynäräinen and O. V. Lounasmaa for useful discussions. This

work was supported by the Academy of Finland and by USSR Academy of Sciences through project ROTA. K. T. and A. J. M. acknowledge scholarships from the Körber and Emil Aaltonen Foundations, respectively.

<sup>1</sup>L. D. Landau Institute for Theoretical Physics, USSR Academy of Sciences, 117334 Moscow, USSR.

<sup>1</sup>J. P. Pekola, K. Torizuka, A. J. Manninen, J. M. Kynnäräinen, and G. E. Volovik, *Phys. Rev. Lett.* **65**, 3293 (1990).

<sup>2</sup>H. K. Seppälä, P. J. Hakonen, M. Krusius, T. Ohmi, M. M. Salomaa, J. T. Simola, and G. E. Volovik, *Phys. Rev. Lett.* **52**, 1802 (1984).

<sup>3</sup>A. L. Fetter, J. A. Sauls, and D. L. Stein, *Phys. Rev. B* **28**, 5061 (1983).

<sup>4</sup>T. Fujita, M. Nakahara, T. Ohmi, and T. Tsuneto, *Prog. Theor. Phys.* **60**, 671 (1978); G. E. Volovik and N. B. Kopnin, *Pis'ma Zh. Eksp. Teor. Fiz.* **25**, 26 (1977); [*JETP Lett.* **25**, 22 (1977)].

<sup>5</sup>P. Hakonen, O. V. Lounasmaa, and J. Simola, *Physica B* **160**, 1 (1989).

<sup>6</sup>N. D. Mermin, in "Quantum Fluids and Solids," eds. S. S. Trickey, E. D. Adams, and J. W. Dufty (Plenum Press, New York, 1979), p. 3.

<sup>7</sup>T.-L. Ho, *Phys. Rev. B* **18**, 1144 (1978).

<sup>8</sup>J. P. Pekola, K. Torizuka, J. M. Kynnäräinen, A. J. Manninen, W. Wojtanowski, and G. K. Tvalashvili, *Europhys. Lett.* **13**, 155 (1990); W. Wojtanowski, private communication.